HHRI report

- Lab 3 -

Z-WIDTH OF THE CONTROLLER

Transparency control and virtual wall

10th September 2024

Students: Killian Raude NX - Jade Therras NX - GROUP 12
Assistants: Giulia Ramella, Jonathan Muheim, Aiden Xu, Mouhamed Zorkot

Contents

1 Notation, figures and tables

θ : position of the paddle (after filtering) $[rad]$
$\dot{\theta}$: speed of the paddle (after filtering) $[rad.s^{-1}]$
R : Reduction ratio of the cable transmission 15[]

Dry friction
$\tau_{stiction}$: static friction torque $[N.m]$
$\overline{\tau}_{stiction}$: average static friction torque $[N.m]$

Viscous friction
$\tau_{viscous}$: viscous friction torque $[N.m]$
B_m : viscous friction coefficient $[N.ms/rad]$
I_{motor} : no load motor current $0.058[A]$
k_{torque} : no load torque constant $0.0346[Nm/A]$
$\dot{\theta}_{noload}$: no load speed of the paddle $670.21[rad.s^{-1}]$

Gravity
$\tau_{gravity}$: torque compensation for the gravity $[N.m]$
m_{paddle} : mass of the paddle $[kg]$
g : gravity constant $6.674 * 10^{-11}[N * m^2 kg^{-2}]$
l_{COM}: length from the point of application to the centre of mass $[m]$

Transparency
$\tau_{transparency}$: torque compensation for the transparency mode $[Nm]$

Virtual wall
τ_{wall} : torque of the motor representing the wall $[N.m]$
θ_{wall}: position of the wall ($\pm$ 0.26) $[rad]$
k : constant of the spring component $[N.s^{-1}]$
B : constant of the damping component $[Nm.s/rad]$
F_{cut} : cut off frequency $[Hz]$
r_{motor} : Motor worm screw radius $[m]$

2 Lists of Figures and Tables

List of Figures

List of Tables

3 Introduction

Haptic interfaces allow users to interact with different virtual environments, notably through touch. Critical aspects of such devices are transparency control and virtual wall rendering. While the prior allows for a more immersive experience for the user by getting rid of the friction of the device for simple motion, the latter allows perception of various virtual interactions as in manipulating real objects.

This Lab report investigates the implementation of such control for the haptic paddle. Transparency control will be implemented by assessing both theoretically and experimentally the different effects opposing motion such as dry and viscous friction as well as the effect of gravity, to aim at compensating them all to facilitate motion. The virtual wall will be rendered as a visco-elastic element that will, on the contrary, oppose motion. The effectiveness of such control will be assessed with K-B plots.

Overall it contributes to the understanding and development of more realistic and immersive haptic experiences by making the user able to feel seemingly frictionless devices that can also render the feel of touching various virtual objects.

4 Identification of the paddle friction

4.1 Static friction torque

Static friction is the friction that exists between a stationary object and the surface on which it's resting. If a force is applied, it should overcome this value for the object to start moving. To identify the static friction, the paddle has been placed in position 0 and a motor torque has been sequentially increased by $0.001[Nm/s]$. The position has been recorded along and plotted in function of the motor torque. As shown in Figure.1.

The experience is noisy and subject to multiple parameters, such as the angle of the paddle (not exactly at 0, change with the help of gravity), the precision of the motor, external friction etc.. The experience has been repeated five times in each direction and the results have been averaged.

In this setup, the value of the motor torque where the first movement is observed and where the paddle starts sliding linearly (the friction is fully overcome) are different, and determine a range for the static dry friction compensation.

In Figure.2, the range is visible. The first value, $\overline{\tau}_{stiction}Minimum$, corresponds to the beginning of the movement of the paddle ($\Delta\theta > 0.1[deg]$). The second value, $\overline{\tau}_{stiction}Maximum$, corresponds to the value of the torque so the paddle starts to move linearly ($\Delta\theta > 0.2[deg]$). The mean of the two values has been chosen for the static dry friction $\overline{\tau}_{stiction}$. Note also that the value of the friction will depend on the direction of the motion.

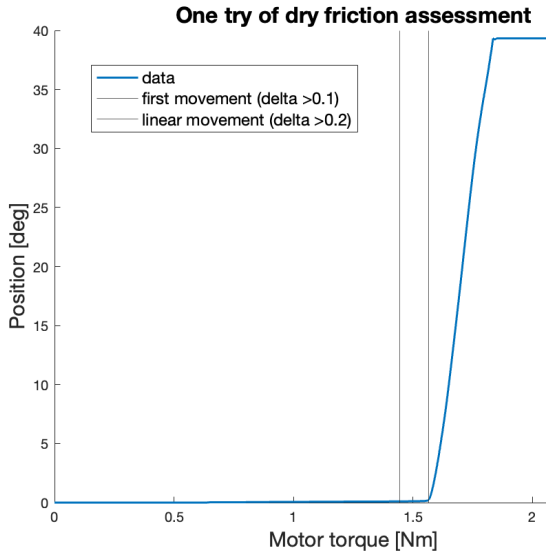

Figure 1: A example of dry friction assessment

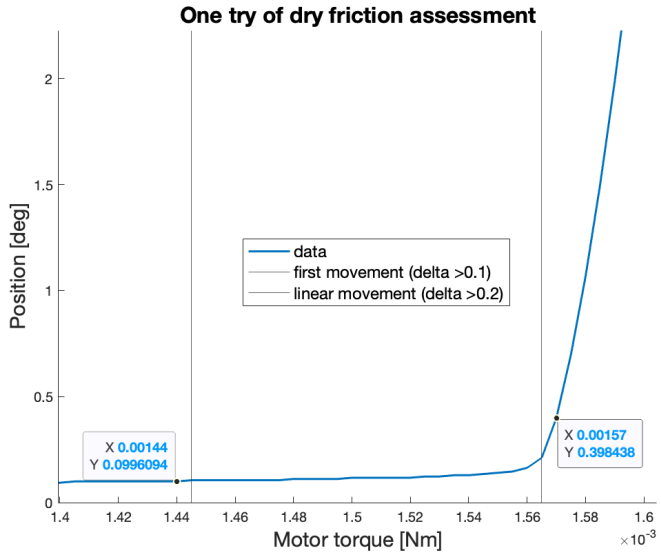

Figure 2: Zoom, dry friction is compensated

Behaviour of the paddle during the dry friction assessment

The instant sliding occurs, the friction is called kinetic (or sliding) friction. As kinetic friction is the force that opposes the relative motion of two surfaces sliding past each other, it is equal to the force that needs to be applied to maintain a constant velocity during the observation period. To determine this value, the speed could be recorded as a function of the motor torque, which is the same experimental setup as before. The experience should start with a constant force, sufficient to make the paddle move (superior to static dry friction). If the paddle starts to accelerate and the velocity increases, the kinetic friction is overcome. The motor torque could be increased sequentially up to this point and the result should be recorded.

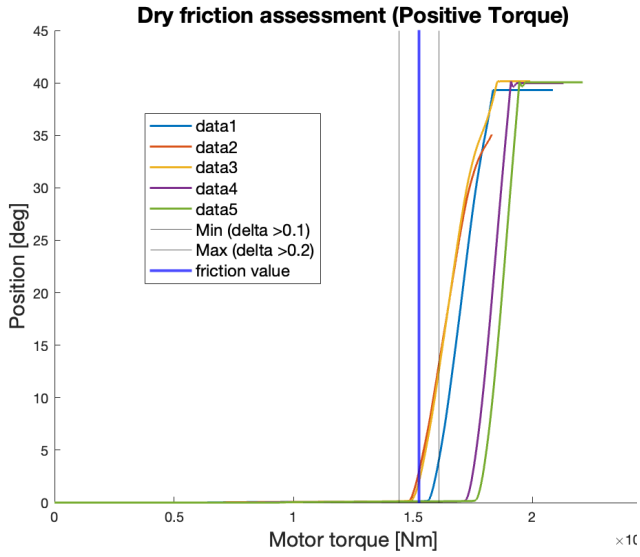

Figure 3: Positive torque

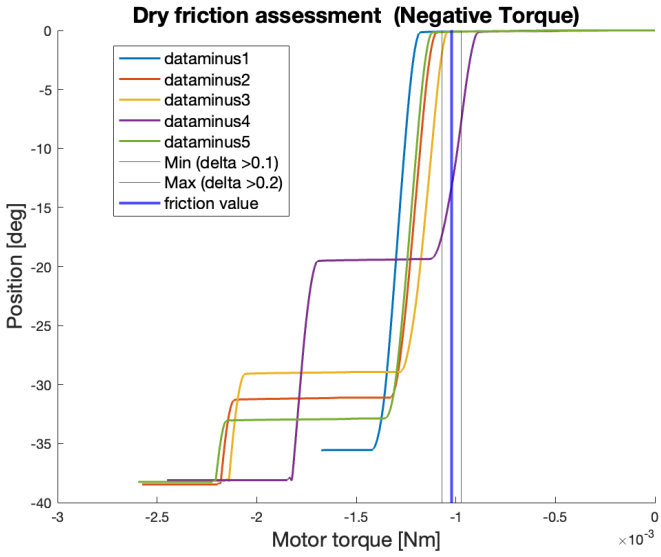

Figure 4: Negative torque

$\overline{\tau}_{stiction} + Minimum : 1.441 * 10^{-3}[Nm]$
standard deviation : $1.022 * 10^{-4}[Nm]$
$\overline{\tau}_{stiction} + Maximum : 1.608 * 10^{-3}[Nm]$
standard deviation : $1.293 * 10^{-4}[Nm]$

$\overline{\tau}_{stiction}+ : 1.525 * 10^{-3}[Nm]$

$\overline{\tau}_{stiction} - Minimum : -0.973 * 10^{-3}[Nm]$
standard deviation : $8.136 * 10^{-5}[Nm]$
$\overline{\tau}_{stiction} - Maximum : -1.071 * 10^{-3}[Nm]$
standard deviation : $1.097 * 10^{-4}[Nm]$

$\overline{\tau}_{stiction}- : -1.022 * 10^{-3}[Nm]$

Response of the paddle to an increasing motor torque

In the positive direction, visualized in Figure.3, the dry friction is compensated with a motor torque of $1.525 * 10^{-3}[Nm]$. With a higher torque value, the paddle starts moving.

In the negative direction, visualized in Figure.4, a plateau is observed, and the first plateau is overcome with a compensation of $-1.022 * 10^{-3}[Nm]$. The observed behaviour could be the result of intern friction in the motor and in the paddle. As it is repeatable, it is not a casual artefact but an intersect property of the paddle.

The dry friction is different between the positive and the negative direction but the order of magnitude is similar, around $10^{-3}[Nm]$, the difference can be attributed to the asymmetrical setting, with the internal friction of the motor and the mounting of the cable being different for the two directions.

The standard deviation is also comparable, around $10^{-4}[Nm]$. This deviation is relatively high as it corresponds to 10% of the friction, highlighting the lack of precision of the experiment.

4.2 Viscous friction torque

Apart from the dry friction, the viscous friction also needs to be compensated. To assess it, the theoretical viscous friction coefficient can be computed at the "no load speed" from the motor data sheet as such :

$$B_m = \frac{I_{motor} * k_{torque}}{\dot{\theta}_{noload}} = 3 * 10^{-6} \tag{1}$$

The viscous friction torque can then be expressed as follows :

$$\tau_{viscous} = \frac{B_m * \dot{\theta}}{R} \tag{2}$$

5 Friction and gravity compensation

5.1 implementation

To implement a transparent control mode of the paddle, the effect of gravity and friction, both dry and viscous, have to be compensated together.

- The dry friction $\tau_{stiction}$, has been identified in the first experiment. The sign of the speed is used to find the direction of motion and a dead zone has been implemented around 0 at $\pm$3rad/sec. The speed can be filtered at a specific cut-off frequency from the GUI to avoid noise and catch the intention of movement. The implementation is shown in Figure.5.

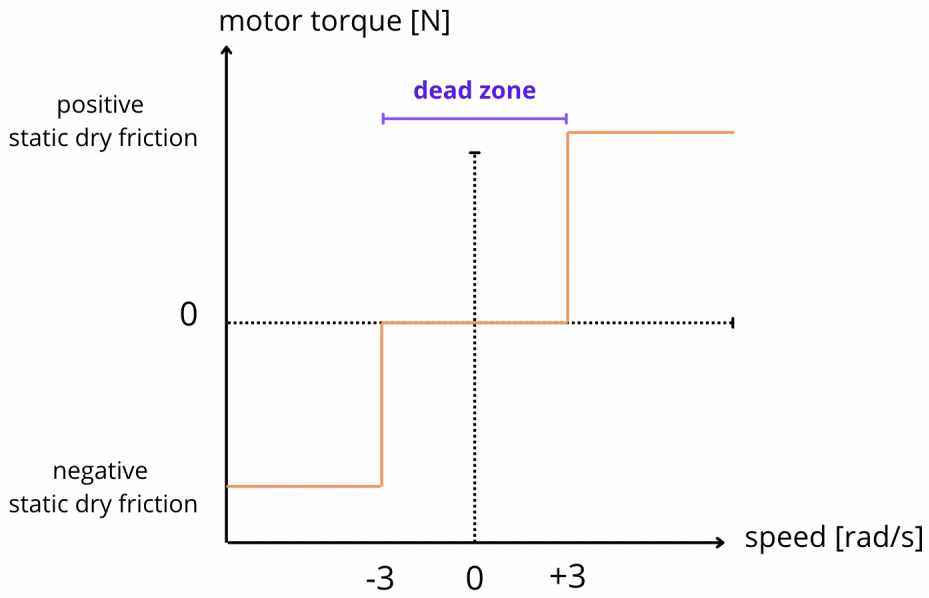

Figure 5: Compensation of the dry friction implementation

Additionally, the static friction is higher than the dynamic friction. The force needed to compensate for the friction before the movement starts is higher than the force needed to compensate for the friction when the paddle is already moving.

- The $\tau_{viscous}$ has been expressed in the previous step. To be accurate, it is important to catch the variation of the speed. The speed is filtered with a specific cut-off frequency for the dry friction.

- The gravity component $\tau_{gravity}$ can be expressed as below. The force of gravity is vertical, acting in the direction of the ground. As the movement of the paddle is constrained to a semi-circle, the impact of gravity depends on the paddle angle.

$$\tau_{gravity} = \frac{m_{paddle} g l_{COM} sin(\Theta)}{R} \tag{3}$$

Overall, the motor torque compensation can be expressed as the sum of the three effect

$$\tau_{transparency} = -\tau_{stiction}(+/-) + \tau_{viscous} + \tau_{gravity} \tag{4}$$

Where $\tau_{stiction}(+/-) = \overline{\tau_{stiction}}+$ if the paddle is moving in the positive direction and $\tau_{stiction}(+/-) = \overline{\tau_{stiction}}-$ if the paddle is moving in the negative direction.

This implementation is called "feed-forward" compensation.
The paddle should behave transparently if a force is applied, no friction should be felt. However, the paddle is also subject to external forces at the entry of the system, impacting the behaviour.
Referring to Figure.6, in this implementation, the compensation is done at the entry of the system, "forward" making it a "feed-forward" compensation.
On the contrary, a "feedback" compensation takes the output of the system and uses it to update the input. In the case of force compensation, an example would be to measure the force applied on the paddle, measure the output movement of the paddle and use the difference between the expected output and the current output to update the input using the motor.

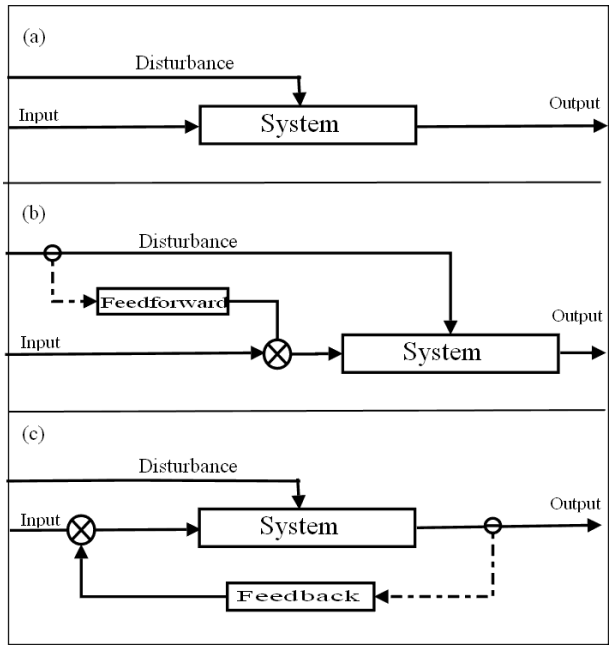

Figure 6: Schematic of feed-forward vs feed-back compensation

Source

In that case, the paddle only has one degree of freedom. In the case of multiple degrees of freedom, the compensation will have to be weighted depending on the direction of the movement. If the robot has multiple actuators for each degree of freedom the compensation could be distributed between each direction.

5.2 Resulting behaviour

To assess the impact of each component, each has been added sequentially. The paddle is moved to describe an oscillation with a constant speed and the motor torque is recorded. The effect of each factor on the motor torque pattern and the feeling of transparency have been assessed and visualized in Figure.10

Compensating only the dry friction results in a step pattern for the motor torque as seen in Figure.7. The correction only depends on the direction of motion. If the movement is really slow, the paddle speed is in the dead zone and no correction is done, hence friction is felt. If there is no dead zone the paddle vibrates around zero speed as the motor torque changes values rapidly back and forth as the speed is noisy. While moving above the dead zone, the effect of the compensation results in a nearly transparent movement. If the paddle is too close to the horizontal position and released, the paddle will fall to the limit. This behaviour is attended to since gravity is still impacting the paddle.

Next, compensation of gravity is added on top of the dry friction. As said, the impact of the gravity depends on the paddle angle. When the paddle approaches the horizontal position (limit of the range) the impact of the gravity will increase, as visible in Figure.8. When moving from the vertical position to the horizontal position, the effect of gravity increases and the compensating motor torque increases as well. The non-linear effect of gravity can be seen added on top of the dry friction correction. Also, when the paddle is not moving, the gravity compensation is still present, preventing the paddle from falling.
With this second component, the paddle feels more transparent, especially in the limit of the range where the effect of gravity is more significant. The movement is fluid and the paddle stays in position if it is stopped independently on the angle. If the paddle is launched at high speed, it is still slowed down by friction.
In the current experience, most of the motor torque compensation depends on the dry friction component, as visualisable in the figure. The gravity component can increase or reduce this value by half depending on the direction.

Finally, viscous friction is compensated as well on top of the two others. The paddle isn't slowed down anymore when the speed of the movement increases. The paddle feels fully transparent no matter the speed, direction and position.
In Figure.9, the impact of this compensation is visible as a little change in the slope across the middle of each step. When the paddle slows down to change direction, the impact of the compensation decreases. In terms of proportion, the viscous effect is much lower than the dry friction and the gravity component due to the very low value of the viscous friction coefficient. Even if its impact increases with the speed of the paddle, it is still the less important factor for transparency compared to the two others.

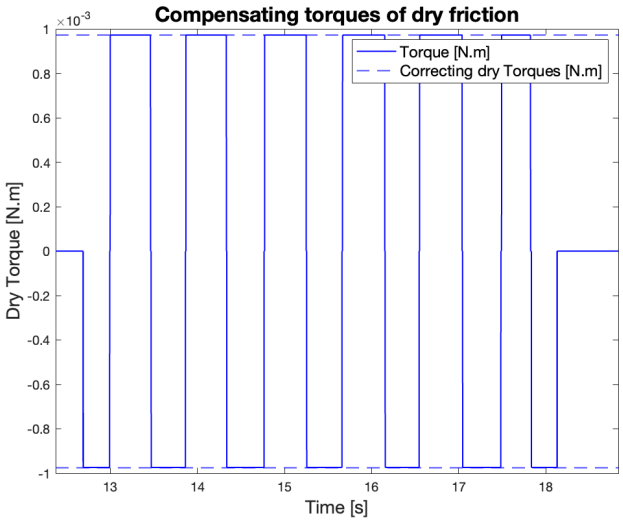

Figure 7: Compensation dry friction

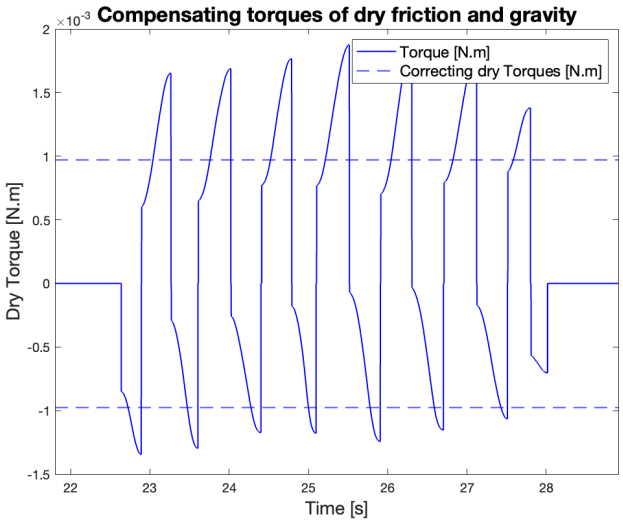

Figure 8: Compensation dry friction + gravity

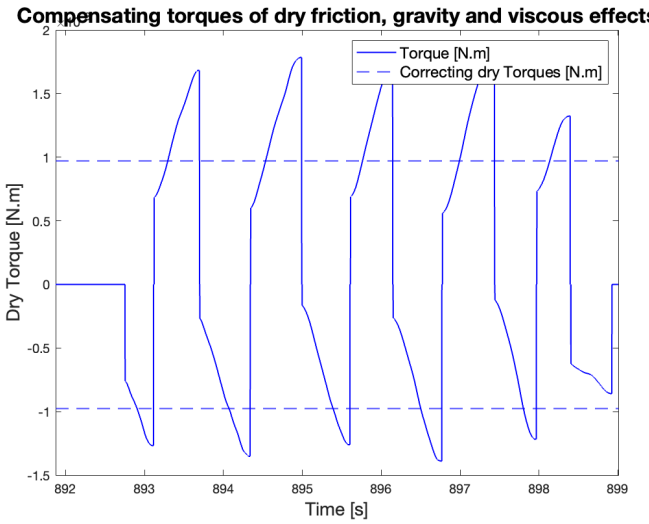

Figure 9: Compensation dry/viscous friction + gravity

Figure 10: Effect of the different compensation with the best set of parameters

6 Virtual wall

6.1 Implementation of the virtual wall

A virtual wall was rendered on top of the transparency control, it follows a visco-elastic behaviour and can be turned on and off from the GUI at $\theta_{wall} \pm 0.26$ $[rad]$ (or $\pm$ 15 $[deg]$). The goal is to be able to have two distinct walls at their predefined position and a transparent control in the middle. In the middle, the motor will apply the same motor torque as before for transparent control, but at θ_{wall} and beyond, the motor torque will change to render the effect of hitting a wall. The equation of the motor torque at this point contains a spring and a damping component. Once more, position and speed can be filtered with a frequency cut F_{cut}.

The motor torque for the wall is computed as such :

$$\tau_{wall} = -\frac{(k * \Delta\theta + B * \dot{\theta}) * r_{motor}}{R} \tag{5}$$

With $\Delta\theta := \theta - \theta_{wall}$ the difference of position.

The parameters k and B can be changed at any time from the GUI.

First, only by rendering the wall with a spring effect by letting the viscous coefficient to zero and increasing the stiffness of the spring, a very stiff wall can be felt at the correct position. Due to the limitations of the applicable motor torque and the system, the wall can be forced and the cable slides around the motor. It is advised to try to stay within an acceptable range of applicable forces to not break the cable and/or paddle. At this point with a high stiffness, coming into the wall too strongly results in the paddle oscillating between the two walls as they push back too strongly in the other way.

However, modifying only the viscosity of the wall results in a highly oscillating pattern at the wall border and a wall that can easily be bypassed if moving into it slow enough which is not wanted.

Tuning both the stiffness and viscosity of the virtual wall accordingly results in the wall opposing motion correctly while not oscillating at the border

6.2 Measurement of the Z-width

An ideal haptic device should be able to deliver a wide range of virtual environments and sensations. In this Lab, both transparency control and a virtual wall were implemented. Both of these behaviours vary in their mechanical impedance, in essence, they relate to how an output force can be generated by an input movement. Transparency control aims at rendering no output force from the initial motion to feel no friction and has hence a theoretical zero mechanical impedance (no resistance to motion), while to hit a wall the mechanical impedance should theoretically be infinite to render a high force at the wall as to not go past it (complete resistance to motion).

A relevant metric to assess the quality of a haptic device is its "Z-width", which represents the dynamic range of mechanical impedance that it can render. The Z-Width of the device can be illustrated as the area under the curve of a K-B plot.

Plots are made for different conditions to compare the effect of the sampling period and the cutoff frequency of the low pass filter on the speed of the range of mechanical impedance that the paddle can render. See Figure 11,12

To take these measures, the viscous effect of the wall is first set to zero and the stiffness is slowly increased until the paddle can be seen oscillating at the wall border when the stiffness is too high. The first point is set as such, then the viscosity is increased stepwise by setting the stiffness to zero and increasing it until oscillations occur again until viscosity alone makes the paddle oscillate. Between 5 and 7 measures are taken to perform the K-B plots.

- **Condition A**: Implementation with transparency control at a sampling period of 350 $[\mu s]$ without filtering of the speed $\dot{\theta}$.
- **Condition B**: Implementation with transparency control at a sampling period of 10 $[ms]$ without filtering of the speed $\dot{\theta}$.
- **Condition C**: Implementation with transparency control at a sampling period of 350 $[\mu s]$ with filtering of the speed $\dot{\theta}$ at 50 Hz.
- **Condition D**: Implementation without transparency control at a sampling period of 350 $[\mu s]$ with filtering of the speed $\dot{\theta}$ at 50 Hz.

Condition A	**First point**	**Second point**	**Third point**	**Fourth point**	**Fifth point**
k	0.6	1.1	1.3	0.8	0.5
B	0	0.0015	0.003	0.0045	0.006

Condition B	**First point**	**Second point**	**Third point**	**Fourth point**	**Fifth point**
k	0.04	0.07	0.09	0.08	0.07
B	0	0.00025	0.0005	0.00075	0.001

Condition C	**First point**	**Second point**	**Third point**	**Fourth point**	**Fifth point**
k	0.5	0.9	1	0.6	0.3
B	0	0.00125	0.0025	0.00375	0.0055

Condition D	**First point**	**Second point**	**Third point**	**Fourth point**	**Fifth point**
k	2.6	3.1	3.6	2.5	1.8
B	0	0.0025	0.005	0.0075	0.01

Table 1: k and B values for assessment of the Z-Width under different conditions.

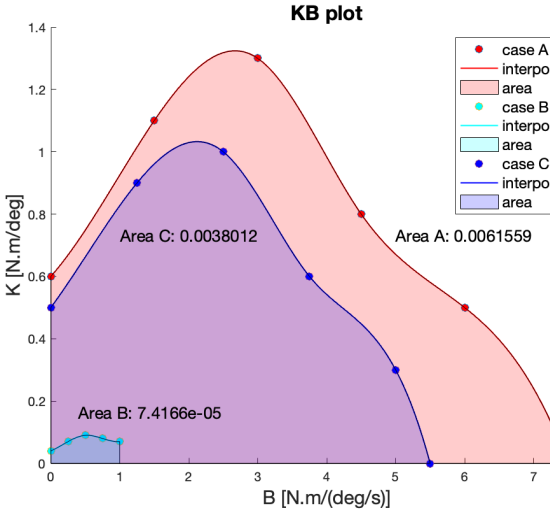

Figure 11: Conditions A B and C

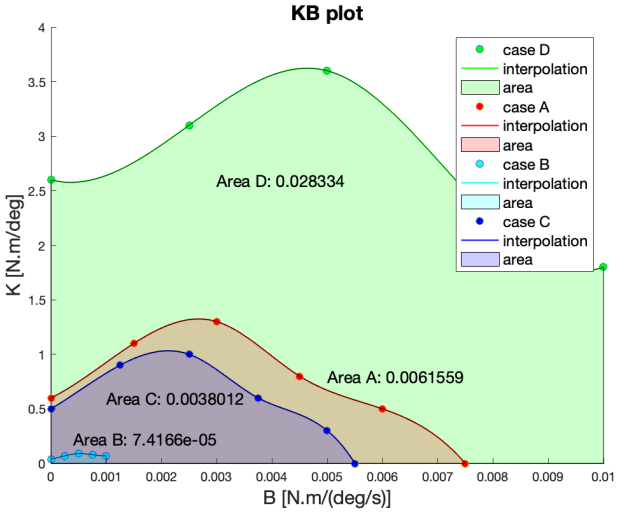

Figure 12: Conditions A B C and D

KB plots for the different conditions in Table:1

6.3 Effect of sampling period and cutoff frequency

When first comparing different sampling period between condition A and B, it becomes apparent that the condition with the lowest sampling period/highest sampling frequency has a bigger Z-width, see Fig.11. The change in resolution offers the most notable effect on the change of the

behavior of the paddle, the region of stability is considerably bigger at high sampling frequencies. This is explainable as the velocity resolution gets worse with higher loop times. For a given motion the difference between two time points will be greater for smaller sampling frequencies and as the delta becomes bigger, the system needs smaller k and B to output the same torque. For a given stable torque, the condition with the smaller deltas can have bigger k and B to compensate them, meaning it can cover a wider range of stable behavior, thus a bigger Z-width. Hence a smaller sampling period leads to small changes in position and velocity from one time point to another and higher k and B before leading to an unstable movement.

While a bigger sampling rate is generally better, offering a better stability of the system over a wider range of mechanical impedance, it also comes with the downside of an increase in computational cost which can saturate the system and introduce delays in computations. At higher sampling rate the noise also become more prominent and can change the fidelity of the designed behavior. The sampling frequency must be high in order to cover a better range of mechanical impedance but reasonable enough as to not saturate the system and amplify the noise.

Next, when comparing conditions A and C with the same sampling period but with C having the speed filtered at 50Hz, it becomes clear that filtering lower the Z-width of the device. This is expected as a low pass filter at a very low cutoff frequency can introduce temporal delays in the system. This will not affect the stiffness rendering on the wall much as this depends on the position which is not filtered, the viscous effect however depends on the filtered speed that will be delayed due to its pass in the filter, as a result the system is less stable.

Overall for each conditions, the motor cannot render both high k and B at the same time, but the range it can covers depends on the sampling frequency and filtering. A high fidelity device needs both a high sampling frequency and proper measures as less noisy as possible that can feed the system without introducing temporal delays through filters.

If the hall sensor was used instead, the system would have suffered dramatically. As both the stiff and viscous effect of the wall rely on precise measure of speed and position, a measure as noisy as the one with the hall sensor would have introduced erratic forces that feel very unstable for the user. Due to noise, both the speed and position measures would bounce between different values and the computed torques would suffer from the inaccurate data reading. A very small Z-width could be expected with oscillations that could happens even for zero stiffness and viscosity of the wall, making the system always unstable.

6.4 Comparison with and without transparency

When implementing the virtual wall without transparent control, obvious changes can be felt in the middle region as the friction is now uncorrected. The most notable change however is situated at the border region, as the resulting force of the wall pushing against motion is directly attenuated by the uncorrected frictions. For a specific set of stiffness and viscosity, the oscillations are bigger for transparent control as they are no friction opposing the oscillations compared to a control without transparent control, see Fig. 14,13. This implementation of the virtual wall without transparent control in the middle also covers most areas in the K-B plot, see Fig.12. This is expected as the oscillations are attenuated by the friction, the wall needs bigger stiffness and viscosity coefficients to overcome friction forces and display an oscillating behaviour at the border. However, while this implementation can deliver a high mechanical impedance it is unable to display a small one at the same time. Indeed while this specific system allows the rendering of more stiffness and viscosity for the wall it is unable to also render a transparent control in the middle region. This is a trade-off that is a design choice and must be discussed depending on the applications and focus of the device.

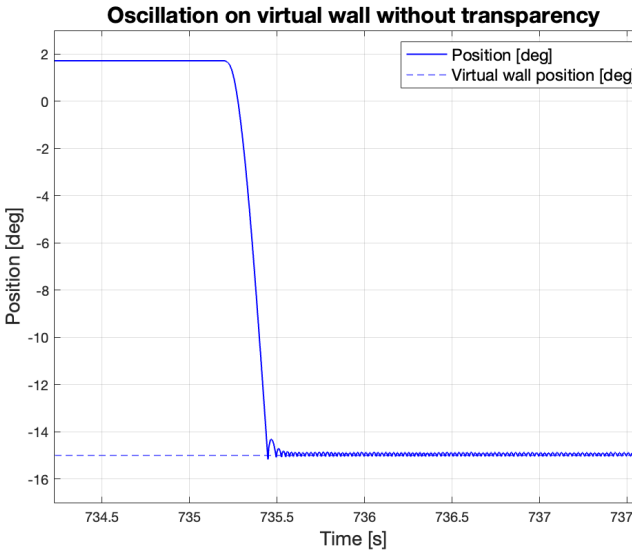

Figure 13: Oscillation without transparency

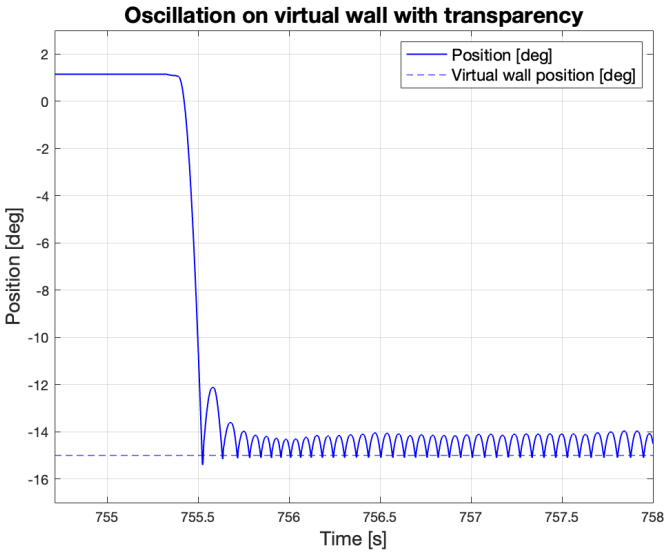

Figure 14: Oscillation with transparency

Oscillation at wall border for the same set of parameters but with and without transparent control in the middle k=4, B=0

7 Conclusion

There are many challenges in rendering virtual environments. While an ideal haptic device would be available to deliver every single haptic feedback and environment from zero to infinite mechanical impedance but also a wide range of temperature, vibrations and more..., there is usually a trade off that specialize the device for a specific utilization.

It has been demonstrated that by assessing the dry and viscous friction of the device as well as the effect of gravity, it was possible to render a transparent feeling to the device. This process could be improved by a better design of the system that would reduce the friction, mostly those of the motor, as well as the addition of a better model of friction that would correct the static and kinetic friction better. A virtual wall can also be rendered, but increasing the mechanical impedance is hindered by keeping the transparent behavior. A bigger Z-width can be achieved by having smooth noiseless measures as well as a high sampling frequency but also by constraining the model to high mechanical impedance and removing the zero impedance behavior.

The ideal haptic device is still far away but these results raise meaningful insight into their functioning and how to go further.